Monochromatic waves in saturated porous materials with anisotropic permeability

Krzysztof Wilmanski

TU Berlin, Sekr. TK7, Str. des 17 Juni 135, 10623 Berlin, Germany

ROSE School Pavia, c/o EUCENTRE, Via Ferrata 1, 27100 Pavia Italy

Abstract

In the paper we investigate the propagation conditions of monochromatic waves in a saturated poroelastic material described by a generalization of Biot's equations. This generalization concerns anisotropic properties of permeability. Mechanical properties of the system are assumed to be described by isotropic constitutive relations but the permeability is given in terms of a tensor of tortuosity. In particular we analyze the propagation in one of the principal directions of this tensor and we show the existence of purely transversal waves for this particular monochromatic wave. We prove the existence of two modes of such waves and investigate their behavior as functions of frequency. A practical application in nondestructive testing of anisotropic materials is indicated.

1 Introduction

Anisotropic properties of porous materials are frequently encountered in biomechanics. This concerns mechanical properties of bones (e.g. [5]) as well as diffusion properties of soft tissues (e.g. [14]). However recent experiments made on various rocks and soils show that these materials possess essentially different diffusion properties in different directions [2, 11] as well and these result from anisotropic tortuosity. The latter notion has been introduced by J. Bear [3] and then developed by means of a statistical analysis of microstructures by J. Bear and Y. Bachmat [4].

An extensive research concerned with anisotropic mechanical properties of two-component porous materials has been carried out by S.C. Cowin [5] and in his recent work with L. Cardoso [6] the wave spectral analysis for such materials is presented. By means of the so-called fabric tensor the set of classical Biot material parameters is extended to cover the case of anisotropic dependence of partial stresses on deformations of both components. However, the permeability remains in this work isotropic in the sense that the flow-resistivity (permeability) tensor is given solely as an isotropic function of the fabric tensor and does not possess anisotropic properties of its own (compare relation (63) in the work [6]).

In spite of the practical importance of the research of Cowin and Cardoso for the description of bones it seems to be not appropriate for the description of a true anisotropic diffusion. We return briefly to this question in Section 3 of this work. Above quoted experiments on rocks indicate that mechanical response of the material is isotropic but the flow is driven by an anisotropic tortuosity. Simultaneously, even though following from geometry of microstructure within a Representative Elementary Volume (REV) these two objects, fabric and tortuosity tensors seem to describe different properties of the true material.

Influence of tortuosity on permeability properties of porous materials has been the subject of research since the early work of J. Kozeny [8]. His formula for the description of diffusivity has been later corrected by Blake and in the form proposed by N. Epstein [7] it is as follows

$$K = \frac{D_h^2 n_0}{b \mu_v \tau^2}, \tag{1}$$

where K denotes the hydraulic conductivity, appearing in Darcy's law, D_h is the hydraulic diameter, n_0 is the initial porosity, μ_v is the true dynamic viscosity of fluid in pores, b is the capillary shape factor (e.g. 32 for circular pores and 48 for parallel slits) and τ denotes the tortuosity. The latter is the fraction of the length of a real streamline between two neighboring points to their distance. It is clear that such a definition does not account for different diffusion conditions in different directions. This was the subject of the model developed by Bachmat and Bear and we use their results in this work.

In this paper we present a few simple results of the wave analysis for saturated porous materials with anisotropic permeability. We use the simplest generalization of Biot's model motivated by the analysis of microstructure of Bear and Bachmat and consider a problem of a transversal wave. Existence of such a wave follows from a particular choice of propagation conditions in this work. The main purpose of this choice is to show that there exist two such modes of propagation and this, in turn, indicates certain new possibilities for a nondestructive testing of porous materials.

2 Governing equations

The two-component model of a porous material considered in this paper is based on a linearity assumption for which the partial balance of momentum equations have the form

$$\rho^S \frac{\partial \mathbf{v}^S}{\partial t} = \operatorname{div} \mathbf{T}^S + \hat{\mathbf{p}}, \quad \rho^F \frac{\partial \mathbf{v}^F}{\partial t} = -\operatorname{grad} p^F - \hat{\mathbf{p}}, \tag{2}$$

where ρ^S, ρ^F are initial constant partial mass densities of skeleton and fluid, respectively, $\mathbf{v}^S, \mathbf{v}^F$ are the partial velocities of these components, $\mathbf{T}^S$ is the partial stress tensor in skeleton and p^F is the partial pressure in fluid. $\hat{\mathbf{p}}$ denotes the momentum source.

Constitutive relations for these quantities are assumed to have the form

$$\begin{aligned} \mathbf{T}^S &= \mathbf{T}_0^S + \lambda^S e \mathbf{1} + 2\mu^S \mathbf{e}^S + Q\varepsilon \mathbf{1}, \quad p^F = p_0^F - Qe - \rho^F \kappa \varepsilon, \\ \hat{\mathbf{p}} &= \hat{p}_i \mathbf{e}_i, \quad \hat{p}_i = \pi_{ij} \left(v_j^F - v_j^S \right), \quad \mathbf{v}^F = v_i^F \mathbf{e}_i, \quad \mathbf{v}^S = v_i^S \mathbf{e}_i, \end{aligned} \tag{3}$$

where $\mathbf{e}_i$ are Cartesian base vectors, $\mathbf{e}_i \cdot \mathbf{e}_j = \delta_{ij}$, $\mathbf{e}^S$ is the Almansi-Hamel small deformation tensor of the skeleton, $e = \operatorname{tr} \mathbf{e}^S, \varepsilon$ are volume changes of skeleton and fluid, respectively. They satisfy the compatibility equations

$$\frac{\partial \mathbf{e}^S}{\partial t} = \mathrm{sym}\,\mathrm{grad}\,\mathbf{v}^S, \quad \frac{\partial \varepsilon}{\partial t} = \mathrm{div}\,\mathbf{v}^F, \tag{4}$$

which, in turn, yield identically partial mass conservation laws for components.

As we consider a linear poroelastic problem in this work changes of porosity are immaterial (compare [13]).

The structure of the permeability tensor (flow-resistivity in terminology of S. C. Cowin) π_{ij} is assumed to be as follows

$$\pi_{ij} = \pi_0 T_{ij}^{-1}, \tag{5}$$

where

$$\pi_0 = \frac{\mu_v b}{D_h^2} \frac{g \rho_0^F}{n_0}, \tag{6}$$

and g is the earth gravity ([14]). The tortuosity tensor $\mathbf{T} = T_{ij}\mathbf{e}_i \otimes \mathbf{e}_j$ is symmetric and it may be interpreted as a static moment of channel openings on the boundary of the Representative Elementary Volume (REV) with respect to a chosen reference point within REV [4]. It can be written in the following spectral form

$$\mathbf{T} = T_{ij}\mathbf{e}_i \otimes \mathbf{e}_j = \frac{1}{\tau^{(3)^2}}\mathbf{n} \otimes \mathbf{n} + \sum_{\mu=1}^{2} \frac{1}{\tau^{(\mu)^2}} \mathbf{m}_\mu \otimes \mathbf{m}_\mu, \tag{7}$$

where $\{\mathbf{n}, \mathbf{m}_1, \mathbf{m}_2\}$ are unit and perpendicular eigenvectors of the tensor $\mathbf{T}$ and $\{\tau^{(1)}, \tau^{(2)}, \tau^{(3)}\}$ are the square roots of inverse eigenvalues of this tensor. We call these quantities principal tortuosities. According to Bear and Bachmat [4] principal tortuosities measure an average inverse of cosines of angles between a short straight interval in a chosen principal direction and a streamline between the endpoints of this interval. Obviously, in the isotropic case they are all equal to τ appearing in Blake-Kozeny relation (1). Hence, similarly to the fabric tensor introduced by Cowin the tortuosity tensor describes purely geometrical properties of the microstructure.

Further we assume the material parameters

$$\left\{\rho^S, \rho^F, \lambda^S, \mu^S, \kappa, Q, \pi_0, \tau^{(1)}, \tau^{(2)}, \tau^{(3)}, \mathbf{n}, \mathbf{m}_1, \mathbf{m}_2\right\}, \tag{8}$$

to be given and constant.

3 Propagation of fronts

In order to see clearly the difference between an influence of anisotropy of stress-strain relations and this of the permeability we reconsider here briefly the field equations of Cowin and Cardoso [6]. They use two unknown fields of displacement $\mathbf{u} = u_i, \mathbf{U} = U_i \mathbf{e}_i$ which are described by the bulk conservation of momentum and the partial balance of momentum for the fluid. These field equations have the following form (equations (31) and (32) in [6])

$$A_{ijkm}\frac{\partial^2 u_k}{\partial x_m \partial x_j} + M_{ij}\frac{\partial^2 w_k}{\partial x_k \partial x_j} = \rho\frac{\partial^2 u_i}{\partial t^2} + \frac{\rho^F}{n_0}\frac{\partial^2 w_i}{\partial t^2}, \tag{9}$$
$$M_{km}\frac{\partial^2 u_k}{\partial x_m \partial x_i} + M\frac{\partial^2 w_k}{\partial x_k \partial x_i} = \frac{\rho^F}{n_0}\left(\frac{\partial^2 u_i}{\partial t^2} + J_{ij}\frac{\partial^2 w_i}{\partial t^2} + \mu_v R_{ij}\frac{\partial w_i}{\partial t}\right),$$

where $\rho = \rho^S + \rho^F$ is the bulk mass density, $\mathbf{u}, \mathbf{w} = \mathbf{U} - \mathbf{u}$ are the dispalcement of the skeleton and the relative displacement, respectively, the material tensors A_{ijkm}, M_{ij}, M are given in terms of the fabric tensor, porosity n_0, true compressibilities and some additional parameters describing anisotropic properties of stress-strain relations. The tensor of inertia J_{ij} is related to the extension of the so-called added mass effect which is immaterial for our considerations. The tensor of flow-resistivity $\mu_v R_{ij}$ and our permeability tesor π_{ij} are identical.

On the front $\mathcal{C}$ of the acoustic wave the following compatibility conditions must be fulfilled

$$[[u_i]] = 0, \quad [[w_i]] = 0, \quad \rho\left[\left[\frac{\partial u_i}{\partial t}\right]\right] = \rho^S\,[[v_i^S]] + \rho^F\,[[v_i^F]] = 0,$$
$$\left[\left[\frac{\partial w_i}{\partial t}\right]\right] = [[v_i^F - v_i^S]] = 0,$$
$$A_i = \left[\left[\frac{\partial^2 u_i}{\partial t^2}\right]\right] = c^2\left[\left[\frac{\partial^2 u_i}{\partial x_k \partial x_m}\right]\right] n_k n_m, \tag{10}$$
$$W_i == \left[\left[\frac{\partial^2 w_i}{\partial t^2}\right]\right] = c^2\left[\left[\frac{\partial^2 w_i}{\partial x_k \partial x_m}\right]\right] n_k n_m,$$

where $[[...]] = (...)^+ - (...)^-$ denotes the jump across the front $\mathcal{C}$. The continuity of displacements, partial mass densities and velocities means that the wave is acoustic while the conditions for amplitudes A_i, W_i follow from Hadamard conditions (e.g. [13]). Obviously, $\mathbf{n} = n_i \mathbf{e}_i$ is the unit vector perpendicular to the front $\mathcal{C}$ and c is the speed of propagation of the front.

Application of the above relations to the field equations (9) yields

$$\left(Q_{ik} - \rho c^2 \delta_{ik}\right) A_k + \left(C_{ik} - \frac{\rho^F}{n_0} c^2 \delta_{ik}\right) W_k = 0, \tag{11}$$
$$\left(C_{ik} - \frac{\rho^F}{n_0} c^2 \delta_{ik}\right) A_k + \left(M\delta_{ik} - \frac{\rho^F}{n_0} J_{ik}\right) W_k = 0,$$

where

$$Q_{ik} = A_{ijkm} n_m n_j, \quad C_{ik} = M_{ij} n_j n_k, \tag{12}$$

are acoustic tensors (compare (54) in [6]). Obviously, relations (11) specify the egenvalue problem whose eigenvalues define the speeds of propagation of various acoustic modes. It is important to notice that the flow resistivity $\mu_v R_{ij}$ has no influence on these speeds. However, the anisotropy of the problem yields more modes of propagation with different speeds than it is the case for isotropic materials. In measuring devices we observe instead of arrivals of classical P1-, S-, P2-modes additional arrivals of pseudotransversal waves.

This is, clearly, also the property of monochromatic waves discussed in the work of Cowin and Cardoso [6].

The situation is different in the case of isotropic stress-strain relations and anisotropy of permeability which we consider in the present work. On the front of acoustic wave we have the following conditions following from equations (2), (3), (4)

$$\begin{aligned} \left(\lambda^S n_i n_j + \mu^S \left(\delta_{ij} + n_i n_j\right) - \rho^S c^2 \delta_{ij}\right) A_j^S + Q n_i n_j A_j^F &= 0, \\ Q n_i n_j A_j^S + \left(\rho^F \kappa n_i n_j - \rho^F c^2 \delta_{ij}\right) A_j^F &= 0, \end{aligned} \tag{13}$$

where

$$A_i^S = \left[\left[\frac{\partial v_i^S}{\partial t}\right]\right], \quad A_i^F = \left[\left[\frac{\partial v_i^F}{\partial t}\right]\right]. \tag{14}$$

Consequently, we have only the arrivals of classical P1-, S-, P2-modes. Anisotropy of permeability has no influence on the structure of acoustic fronts. It has only an influence on speeds of monochromatic waves as we show further in this work.

The above presented difference has an important practical bearing. For waves of very high frequency the number of arrivals will be bigger for anisotropic stress-strain relations than the number of arrivals for anisotropic permeability alone. This allows to distinguish these two cases experimentally.

4 Monochromatic waves

We investigate the propagation of monochromatic waves of a given frequency ω, i.e. we seek solutions of the governing equations in the following form

$$\begin{aligned} \mathbf{v}^S &= \mathbf{V}^S \mathcal{E}, \quad \mathbf{v}^F = \mathbf{V}^F \mathcal{E}, \quad \mathbf{e}^S = \mathbf{E}^S \mathcal{E}, \quad \varepsilon = E^F \mathcal{E} \\ \mathcal{E} &= e^{i(\mathbf{k}\cdot\mathbf{x} - \omega t)} \equiv e^{-((\operatorname{Im} k)\mathbf{n}\cdot\mathbf{x})} e^{i \operatorname{Re} k \left(\mathbf{n}\cdot\mathbf{x} - c_{ph} t\right)}, \\ \mathbf{k} &= k\mathbf{n}, \quad \mathbf{n}\cdot\mathbf{n} = 1, \quad c_{ph} = \frac{\omega}{\operatorname{Re} k}. \end{aligned} \tag{15}$$

where $\mathbf{V}^S, \mathbf{V}^F, \mathbf{E}^S, E^F$ are constant amplitudes, $\mathbf{k}$ is the wave vector, k is the wave number, $\mathbf{n}$ denotes the direction of propagation and c_{ph} is the speed of propagation of the monochromatic wave of frequency ω.

Compatibility equations (4) yield

$$\mathbf{E}^S = -\frac{1}{2\omega}\left(\mathbf{V}^S \otimes \mathbf{k} + \mathbf{k} \otimes \mathbf{V}^S\right), \quad E^F = -\frac{1}{\omega}\mathbf{V}^F \cdot \mathbf{k}. \tag{16}$$

Bearing in mind the momentum balance equations (2) and the constitutive relations (3), (5) we arrive at the following set of algebraic relations

$$\begin{gathered} \left(-\rho^S \omega^2 \mathbf{1} + \lambda^S \mathbf{k} \otimes \mathbf{k} + \mu^S \left(k^2 \mathbf{1} + \mathbf{k} \otimes \mathbf{k}\right) - i\pi_0 \omega \mathbf{T}^{-1}\right) \mathbf{V}^S + \\ + \left(Q\mathbf{k} \otimes \mathbf{k} + i\pi_0 \omega \mathbf{T}^{-1}\right) \mathbf{V}^F = 0, \\ \\ \left(Q\mathbf{k} \otimes \mathbf{k} + i\pi_0 \omega \mathbf{T}^{-1}\right) \mathbf{V}^S + \\ + \left(-\rho^F \omega^2 \mathbf{1} + \rho^F \kappa \mathbf{k} \otimes \mathbf{k} - i\pi_0 \omega \mathbf{T}^{-1}\right) \mathbf{V}^F = 0. \end{gathered} \tag{17}$$

Obviously, this is the eigenvalue problem for the amplitudes of the waves. In this paper, we investigate only a very particular special form of this set. This is the subject of the next Section.

5 Transversal waves

We have made already the assumption that the tortuosity tensor is constant. Consequently, its eigenvectors $\{\mathbf{n}, \mathbf{m}^1, \mathbf{m}^2\}$ can be chosen as global base vectors of the Cartesian frame of reference. Then the amplitudes of velocities can be written in the form

$$\mathbf{V}^S = V^{S\|}\mathbf{n} + \sum_{\mu=1}^{2} V_\mu^{S\perp}\mathbf{m}_\mu, \quad \mathbf{V}^F = V^{F\|}\mathbf{n} + \sum_{\mu=1}^{2} V_\mu^{F\perp}\mathbf{m}_\mu. \tag{18}$$

We show that the system (17) admits the solution for which

$$\mathbf{k} = k\mathbf{n}, \quad V^{S\|} = 0, \quad V^{F\|} = 0, \tag{19}$$

where k is the wave number. We call this solution a transversal wave.

Substitution of the assumption (19) in the set (17) yields

$$\begin{gathered}\left(-\rho^S\omega^2\mathbf{1}+\mu^S k^2\mathbf{1} - i\omega\pi_0\sum_{\mu=1}^{2}\tau^{(\mu)^2}\mathbf{m}_\mu\otimes\mathbf{m}_\mu\right)\sum_{\nu=1}^{2}\mathbf{m}_\nu V_\nu^{S\perp}+ \\ +\left(i\pi_0\omega\sum_{\mu=1}^{2}\tau^{(\mu)^2}\mathbf{m}_\mu\otimes\mathbf{m}_\mu\right)\sum_{\nu=1}^{2}\mathbf{m}_\nu V_\nu^{F\perp} = 0, \\ \left(i\pi_0\omega\sum_{\mu=1}^{2}\tau^{(\mu)^2}\mathbf{m}_\mu\otimes\mathbf{m}_\mu\right)\sum_{\nu=1}^{2}\mathbf{m}_\nu V_\nu^{S\perp}+ \\ +\left(-\rho^F\omega^2\mathbf{1} - i\omega\pi_0\sum_{\mu=1}^{2}\tau^{(\mu)^2}\mathbf{m}_\mu\otimes\mathbf{m}_\mu\right)\sum_{\nu=1}^{2}\mathbf{m}_\nu V_\nu^{F\perp} = 0,\end{gathered} \tag{20}$$

where the inverse of the spectral representation (7) of the tortuosity tensor has been used. Orthogonality of eigenvectors leads to the following two sets of algebraic relations

$$\begin{gathered}\left(-\omega^2 + \frac{\mu^S}{\rho^S}k_\nu^2 - \frac{i\pi_0\omega}{\rho^S}\tau^{(\nu)2}\right)V_\nu^{S\perp} + \frac{i\pi_0\omega}{\rho^S}\tau^{(\nu)2}V_\nu^{F\perp} = 0, \\ \frac{i\pi_0\omega}{\rho^F}\tau^{(\nu)2}V_\nu^{S\perp} - \left(\omega^2 + \frac{i\pi_0\omega}{\rho^F}\tau^{(\nu)2}\right)V_\nu^{F\perp} = 0, \quad \nu = 1,2.\end{gathered} \tag{21}$$

For distinct tortuosities $\tau^{(1)}$ and $\tau^{(2)}$ there exist two solutions of this set, i.e. two modes of propagation: either

$$\begin{gathered}\left(\omega^2 - \frac{\mu^S}{\rho^S}k_1^2 + \frac{i\pi_0\omega}{\rho^S}\tau^{(1)^2}\right)\left(\omega^2 + \frac{i\pi_0\omega}{\rho^F}\tau^{(1)^2}\right) + \\ +\frac{\rho^F}{\rho^S}\left(\frac{\pi_0\omega}{\rho^F}\tau^{(1)^2}\right)^2 = 0, \quad V_1^{S\perp} \neq 0, \quad V_1^{F\perp} \neq 0,\end{gathered} \tag{22}$$

and then $V_2^{S\perp}=0, \quad V_2^{F\perp}=0$, or

$$\left(\omega^2-\frac{\mu^S}{\rho^S}k_2^2+\frac{i\pi_0\omega}{\rho^S}\tau^{(2)^2}\right)\left(\omega^2+\frac{i\pi_0\omega}{\rho^F}\tau^{(2)^2}\right)+$$
$$+\frac{\rho^F}{\rho^S}\left(\frac{\pi_0\omega}{\rho^F}\tau^{(2)^2}\right)^2=0, \quad V_2^{S\perp}\neq 0, \quad V_2^{F\perp}\neq 0, \tag{23}$$

and then $V_1^{S\perp}=0, \quad V_1^{F\perp}=0$. Both modes have amplitudes perpendicular to the direction of propagation $\mathbf{n}$. Dispersion relations (22), (23) can be written in the following convenient form

$$\omega\left(\omega^2-\frac{\mu^S}{\rho^S}k_\nu^2\right)+ \tag{24}$$
$$+i\pi_0\tau^{(\nu)^2}\frac{\rho^S+\rho^F}{\rho^S\rho^F}\left(\omega^2-\frac{\mu^S}{\rho^S+\rho^F}k_\nu^2\right)=0, \quad \nu=1,2.$$

For equal principal tortuosities $\tau^{(1)}=\tau^{(2)}$ this result is identical with the result for isotropic permeability [1]. In the limit of very low and and very high frequencies it yields the following phase speeds of propagation

$$\lim_{\omega\to 0}\frac{\omega}{\operatorname{Re}k_\nu}=\sqrt{\frac{\mu^S}{\rho^S+\rho^F}}, \quad \lim_{\omega\to\infty}\frac{\omega}{\operatorname{Re}k_\nu}=\sqrt{\frac{\mu^S}{\rho^S}}, \quad \nu=1,2. \tag{25}$$

respectively. Hence these speeds are the same for both modes and coincide with the well-known results of the wave analysis for soils.

The existence of the pure transversal modes is not typical for anisotropic materials. This results from a very strong assumption that the propagation direction $\mathbf{n}$ coincides with one of the principal directions of the constant tortuosity tensor. Otherwise, it can be shown that longitudinal and transversal modes do not exist in the pure form and, in addition, there exists a coupling of pseudotransversal modes through the Biot coupling constant Q. We shall not present these problems in this short note.

6 Phase speeds and attenuations

Dispersion relation (24) can be easily solved with respect to the wave number. We obtain

$$k_\nu^2=\frac{\omega_0^2}{c_\infty^2}\frac{(\omega/\omega_0)^2}{(\omega/\omega_0)^2+\tau^{(\nu)^4}}\left[(\omega/\omega_0)^2+ir\tau^{(\nu)^2}(\omega/\omega_0)+(1+r)\,\tau^{(\nu)^4}\right], \tag{26}$$

where

$$\omega_0=\frac{\pi_0}{\rho^F}, \quad c_\infty^2=\frac{\mu^S}{\rho^S}, \quad r=\frac{\rho^F}{\rho^S}. \tag{27}$$

This relation yields immediately phase velocities and attenuations of monochromatic waves

$$c_{ph}^\nu=\frac{c_\infty\sqrt{2}}{\sqrt{A_\nu+\sqrt{A_\nu^2+B_\nu^2}}}, \quad \operatorname{Im}k_\nu=\frac{\omega_0}{c_\infty\sqrt{2}}\frac{(\omega/\omega_0)\,B_\nu}{\sqrt{A_\nu+\sqrt{A_\nu^2+B_\nu^2}}}, \tag{28}$$

where

$$A_\nu = \frac{1}{(\omega/\omega_0)^2 + \tau^{(\nu)^4}} \left[(\omega/\omega_0)^2 + (1+r)\,\tau^{(\nu)^4} \right],$$

$$B_\nu = \frac{r\tau^{(\nu)^2}\,(\omega/\omega_0)}{(\omega/\omega_0)^2 + \tau^{(\nu)^4}}. \tag{29}$$

Hence, in the limits of low and high frequency we obtain phase velocities given by relation (25) and the limits of attenuation are as follows

$$\lim_{\omega\to 0} \operatorname{Im} k_\nu = 0, \quad \lim_{\omega\to\infty} \operatorname{Im} k_\nu = \frac{r\omega_0\tau^{(\nu)^2}}{2c_\infty} = \frac{\pi_0\tau^{(\nu)^2}}{2\sqrt{\mu^S\rho^S}}. \tag{30}$$

As expected the attenuation grows in square of the tortuosity which indicates an importance of this parameter in the description of waves. The behavior of both functions c_{ph}^ν and $\operatorname{Im} k_\nu$ of frequency ω is monotonous. Below we demonstrate a numerical example.

7 Numerical example

In order to appreciate the frequency dependence of speeds and attenuations we consider a numerical example for which we use the following data

$$\begin{aligned}
K_s &= 48 \;\; [\text{GPa}], \quad \nu = 0.2, \quad n_0 = 0.3, \\
\rho^{SR} &= 2500 \;\; [\text{kg/m}^3], \quad \text{i.e.} \quad \rho^S = 1750 \;\; [\text{kg/m}^3] \\
r &= 0.1714, \quad \pi_0 = 10^{10} \;\; [\text{kg/m}^3\text{s}], \\
\tau^{(1)} &= 1.06, \quad \tau^{(2)} = 6.50.
\end{aligned} \tag{31}$$

where K_s is the true compressibility modulus of the material and ν is the Poisson number. True and partial mass densities of the skeleton are connected by the relation $\rho^S = (1-n_0)\,\rho^{SR}$. These data correspond roughly to Alermoehe sandstone saturated by water and it was investigated by a mobile NMR device by J. Arnold [2]. Then the Gassmann and Geertsma relations (e.g. [1]) yield

$$\begin{aligned}
\mu^S &= \frac{3}{2}\frac{1-2\nu}{1+\nu}\frac{K_s}{1+50n_0} = 2.25 \;\; [\text{GPa}], \\
c_\infty &= 1134 \;\; [\text{m/s}], \quad \omega_0 = 33.3 * 10^6 \;\; [1/\text{s}].
\end{aligned} \tag{32}$$

In the work [2] the values of tortuosity vary in the interval indicated by the data (31). However, there is no direct information on anisotropy of the structure. This may be only suspected because samples were extracted from a very similar depth, reported values of porosity are similar and variations in permeability seem to be related to variations of tortuosity. Similar conclusions follow from the work [11] in which the values of tortuosity for various rocks vary between 3.45 and 7.69.

According to (28), the frequency limits of phase speeds and attenuations for both transversal modes are as follows

$$
\begin{gathered}
\lim_{\omega\to 0} c_{ph}^1 = \lim_{\omega\to 0} c_{ph}^2 = 1048 \quad [\mathrm{m/s}], \\
\lim_{\omega\to 0} \operatorname{Im} k_1 = \lim_{\omega\to 0} \operatorname{Im} k_2 = 0, \\
\lim_{\omega\to \infty} c_{ph}^1 = \lim_{\omega\to \infty} c_{ph}^2 = 1134 \quad [\mathrm{m/s}], \\
\lim_{\omega\to \infty} \operatorname{Im} k_1 = 2831 \quad [1/\mathrm{m}], \quad \lim_{\omega\to 0} \operatorname{Im} k_2 = 106460 \quad [1/\mathrm{m}].
\end{gathered} \tag{33}
$$

These values indicate an enormous influence of tortuosity on the attenuation. In contrast to the first transversal mode the second one is practically not measurable in the range of high frequencies due to the high value of $\tau^{(2)}$.

In Figures below we show the behavior of both characteristic quantities of waves for a very large interval of frequency in order to indicate their asymptotic properties. The frequency and the attenuation are normalized in the following way

$$
\begin{aligned}
\omega &\rightarrow \omega/\omega_0, \quad \omega_0 = 33.3 * 10^6 \quad [1/\mathrm{s}], \\
\operatorname{Im} k_\nu &\rightarrow \frac{c_\infty\sqrt{2}}{\omega_0} \operatorname{Im} k_\nu, \quad \frac{c_\infty\sqrt{2}}{\omega_0} = 0.4816 * 10^5 \quad [\mathrm{m}].
\end{aligned} \tag{34}
$$

In Figure 1 we show the plots of phase velocities for frequency ω up to app. 10^8 [1/s]. For very low frequencies both speeds are almost constant and possess the value 1048 [m/s] indicated in (33). Then they begin to grow for both tortuosities but the growth for higher eigenvalue of tortuosity $\tau^{(2)} = 6.50$ is slower than for the lower value. In the range of very high frequencies they converge to the same limit value 1134 [m/s]. This is shown again in Fig. 2 and, obviously, it is a consequence of the hyperbolicity of the system for which the limit value becomes the speed of front.

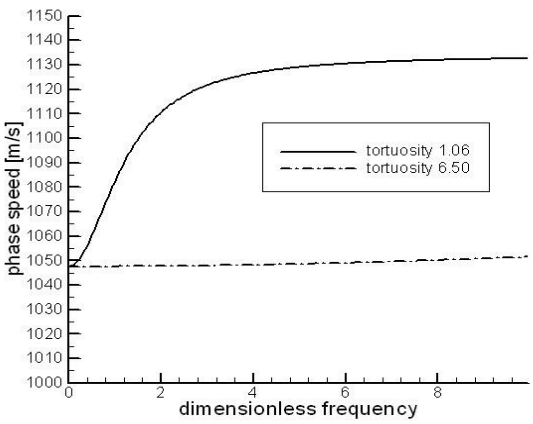

Fig. 1: *Phase speed c_{ph}^ν [m/s] of monochromatic waves in function of dimensionless frequency ω/ω_0 for principal tortuosities $\tau^{(1)} = 1.06$ (solid line) and $\tau^{(2)} = 6.5$ (dotted line)*

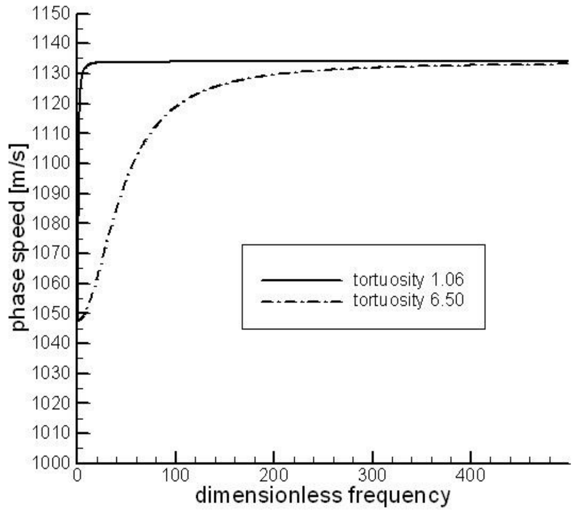

Fig. 2: *Phase speed* c^{ν}_{ph} [m/s] *of monochromatic waves for large frequency range for principal tortuosities* $\tau^{(1)} = 1.06$ *(solid line) and* $\tau^{(2)} = 6.5$ *(dotted line)*

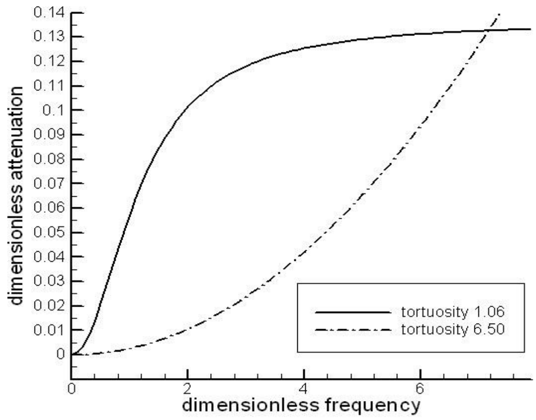

Fig. 3: Dimensionless *attenuation* $\left(\frac{c_\infty\sqrt{2}}{\omega_0}\,\mathrm{Im}\,k_\nu\right)$ *of monochromatic waves in function of dimensionless frequency* ω/ω_0 *for principal tortuosities* $\tau^{(1)} = 1.06$ *(solid line) and* $\tau^{(2)} = 6.5$ *(dotted line)*

In Fig. 3 we see a peculiar behavior of attenuation for relatively low frequencies. Namely, in spite of a larger resistance to the diffusive flow for higher values of tortuosity the attenuation of monochromatic waves is smaller for large eigenvalue of tortuosity $\tau^{(2)} = 6.50$ than for the low value $\tau^{(1)} = 1.06$. It is only for very high frequencies where the attenuation of waves for higher values of tortuosities becomes larger (106460 [1/m] in the limit $\omega \to \infty$) than this for lower values of tortuosity (2831 [1/m] in the limit $\omega \to \infty$). We show this behavior for low frequencies (up to app. 500 [kHz]) in Fig. 4.

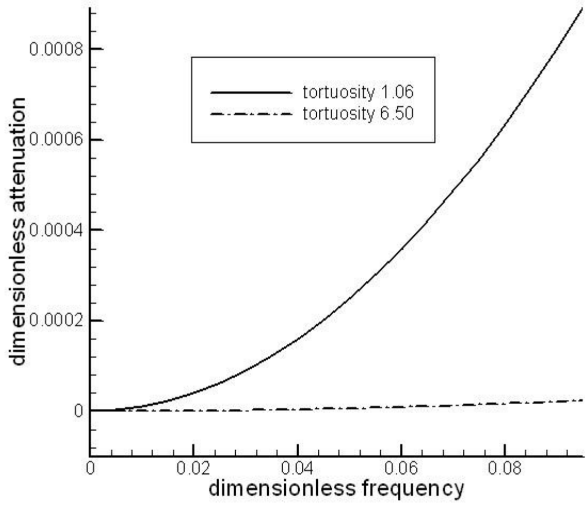

Fig. 4: Dimensionless *attenuation* $\left(\frac{c_\infty\sqrt{2}}{\omega_0}\,\mathrm{Im}\,k_\nu\right)$ *of monochromatic waves for low frequencies for principal tortuosities* $\tau^{(1)} = 1.06$ *(solid line) and* $\tau^{(2)} = 6.5$ *(dotted line)*

This is similar to the properties of monochromatic waves in isotropic materials with different permeabilities. As indicated, for instance, in the work of Wilmanski and Albers [12] the attenuation curves for S-waves for different permeabilities intersect each other (compare Fig. 9 in [12]). This property can be used in the experimental measurements of anisotropic properties of tortuosity and, consequently, the permeability. The low frequency waves in the direction of low tortuosity arrive earlier and they are stronger attenuated than these in the direction of high tortuosity.

8 Conclusions

Even though presented only for a very special choice of propagation conditions transversal waves in poroelastic media with anisotropic permeability indicate a property very important for practical applications. It is well known that such an anisotropy yields also an important correction of the equation for magnetization known as the Bloch-Torrey equation. This equation forms the basis of the Magnetic Resonance Imaging (MRI), a tool for the modern diagnosis in medicine. Anisotropy of the diffusion measured by this method yields, for instance, an information on various diseases of brain [9], [10]. Anisotropic properties of acoustic waves can deliver a similar information on the image of microstructure of soils and rocks. In particular, transversal waves, or waves similar to them in a general case of propagation, are easily measurable and a distinction of their modes yields a direct information on the structure of the tortuosity tensor. As this tensor determines the permeability it has a great practical bearing for such structures as tunnels, embankment dams and road construction in which the intensity and directions of seepage processes play an important role.

References

[1] B. Albers, K. Wilmanski; Modeling acoustic waves in saturated poroelastic media, *Jour. of Engn. Mechanics*, ASCE, **131**, 974-985, 2005.

[2] J. Arnold; *Mobile NMR for Rock porosity and permeability*, PhD-Thesis, RWTH Aachen, 2007.

[3] J. Bear; *Dynamics of Fluids in Porous Media*, Dover, N.Y. 1988.

[4] J. Bear, Y. Bachmat; *Introduction to Modeling of Transport Phenomena in Porous Media*, Kluwer, Dordrecht, 1991.

[5] S. C. Cowin; Bone poroelasticity, *J. Biomech,* **32,** 218-238.

[6] S. C, Cowin, L. Cardoso; Fabric dependence of wave propagation in anisotropic porous media, *Biomech Model Mechanobiol*, **10**, 39-65, 2011.

[7] N. Epstein; On tortuosity and the tortuosity factor in flow and diffusion through porous media, *Chem. Engn. Sci.*, **44**, 3, 777-779, 1989.

[8] J. Kozeny; Über kapillare Leitung des Wassers in Boden(Aufstieg, Versickerung und Anwendung auf Bewässerung), *Sber. Akad. Wiss.*, Wien, **136**, (Abt. IIa), 271-306, 1927.

[9] Y. Masutani, S. Aoki, O. Abe, N. Hayashi, K. Otomo; MR diffusion tensor imaging: recent advance and new techniques for diffusion tensor visualization, *European Jour. Radiology*, **46**, 53-66, 2003.

[10] D. A. Rusakov, D. M. Kullmann, Geometric and viscous components of the tortuosity of the extracellar space in the brain, *Proc. Natl. Acad. Sci. USA, Neurobiology,* **95**, 8975-8990, 1998.

[11] R. Wang, T.Pavlin, M. S. Rosen, R. W. Mair, D. G. Cory, R. L. Walsworth; Xenon NMR measurements of permeability and tortuosity in reservoir rocks, *Magn. Res. Im.* 1-9, 2004.

[12] K. Wilmanski, B. Albers; Acoustic waves in porous solid-fluid mixtures, in: *Dynamic Response of Granular and Porous Materials under Large and Catastrophic Deformations*, K. Hutter, N. Kirchner (eds.), Springer, Berlin, 285-313, 2003.

[13] K. Wilmanski; *Continuum Thermodynamics. Part I. Foundations*, World Scientific, New Jersey, 2008.

[14] K. Wilmanski; Permeability, tortuosity, and attenuation of waves in porous materials, *Civil and Environmental Engineering Research (* CEER), Zielona Gora, **5**, 9-52, 2010.